

Fine Structure of Fluorinated Copolymer / Nono-filler Composites

Yuichiro Hayasaka, Tadashi Tamura, and Atsuhiko Fujimori*

Graduate School of Science and Engineering, Yamagata University, Yonazawa, Yamagata, 992-8510, Japan

Fax: +81-238-26-3073, e-mail: fujimori@yz.yamagata-u.ac.jp

Fine structure in the matrix polymer and dispersion state of fillers for poly [tetrafluoroethylene-co-(perfluoroalkylvinylether)] (*abbrev.* PFA) / nano-fillers (such as organo-modified smectite, organo-modified mica, and porous silica particles) composites were investigated by wide-angle X-ray diffraction (WAXD), small-angle X-ray scattering (SAXS), transmission electron microscopy (TEM), and differential scanning calorimetry (DSC).

From the results of TEM observation, it was found that nano-fillers were almost uniformly dispersed in PFA matrix. Further, PFA / nano-filler composites are exhibited relatively larger distance between lamellar gravity at least 30 nm estimated by SAXS than general hydrogenated crystalline polymer. This result means that fluorinated copolymer formed the thicker lamella crystal. In addition, a melting peak these nanocomposites showed in DSC thermograms was shifted to higher temperature side than that of neat PFA. It is suggested that the origin of this thermal behavior corresponds to occurrence the nucleator effect of nano-fillers to the matrix PFA.

Key words: fluorinated copolymer, nanocomposites, wide-angle X-ray diffraction, small-angle X-ray scattering, transmission electron microscopy

1. INTRODUCTION

In recent years, polymer/clay composites (polymer / clay hybrids, abbreviated to PCHs) have attracted much attention as a new class of polymer-based composites, offering high potentials for ever-expanding versatile application.^{1,2} The term PCHs represents composite composed of a matrix polymer couple, with a small percentage of clay minerals of nanometer in thickness and several micrometers in size. Compared with conventional composites that contain fillers of millimeter or micrometer size, the loading of exfoliated layered clay imparts excellent properties to the matrix, such as high dimensional stability, gas barrier performance, high heat deflection temperature, and flame retardancy in addition to reinforced mechanical properties.³

The well-known technologies for PCHs production are broadly classified as *intercalative polymerization and as direct blending or melt compounding* of clay into polymer matrix.^{1,2} The former consists of first dispersing organo-modified clay particles in a monomer liquid from which some monomer molecules may be absorbed (intercalated) into the clay galleries and of subsequent polymerization of the monomer under suitable conditions.⁴ The latter is compounding of an organo-modified clay into a polymer matrix from either solution⁵ or melt.⁶ Vaia *et al*⁷ have reported the kinetics of polymer melt intercalation for polystyrene/clay hybrid system.

To improve the gas barrier performance and mechanical properties PCHs, a uniformly exfoliated clay structure obtained in the matrix is necessary. However, this process so far has encountered difficulties because of the quite weak clay-polymer interaction against the hindrance electrostatic clay-clay attraction. To achieve a good dispersion and/or delamination of

clay, there are at least two controlling factors: One is due to the chemical nature, such as high clay-polymer interaction, and the other is due to the processing condition, such as high-shear melt-mixing.⁸ The improvement of the interaction between naturally hydrophilic clay and usually more or less hydrophobic polymer can be quite effectively achieved by hydrophobic modification of the clay with a suitable alkyl-ammonium surfactant and/or direct hydrophilic modification of the polymer by introducing more highly polar groups. Although such PCHs certainly have high potential for versatile future applications, there are serious drawbacks due to their environmental incompatibility arising from their matrix polymers. The blending or hybridization with clay minerals makes them more difficult to handle, yielding undegradable PCHs waste.

On the other hands, poly[tetrafluoroethylene-co-[perfluoropropylalkylvinylether]] (PFA)⁹ has a unique role in the plastics industry due to its inertness, heat resistance, and low coefficient of friction in a wide temperature range. Generally, fluorinated compounds and fluoropolymers have excellent chemical resistance, oil resistance, and oil- and water-shedding resistance.¹⁰ They have been used as rubbers at high temperatures and as several lubricating fluorine manufactured products. However, in the field of fundamental science, the structural studies on fluorinated polymers have progressed slowly since first reported by Bunn and Howells in 1954.¹¹ We also found very few reports on the systematic studies on the fluorinated copolymer and their composites because these compounds are difficult to synthesize due to the emission of poisonous gases.¹²

In this study, the fine structure of PFA matrix in hybrid and dispersed state of clay particles are characterized by use of wide-angle

X-ray diffraction (WAXD), transmission electron microscopy (TEM), and small-angle X-ray scattering (SAXS). The preliminary information on PFA crystallite morphology of PFA/clay hybrids obtained by WAXD is also reported.

2. EXPERIMENTAL

2.1 Materials and preparation of samples

The organophilic clay, prepared by an ion exchange reaction of between a purified Na^+ -smectite or -mica, and dimethyl dioctadecyl phosphate, was kindly supplied by Technical Center, DuPont-Mitsui Fluorochemicals Co. Ltd. Also, the poly[tetrafluoroethylene-co-(perfluoro-alkylvinylether)] (PFA) used in this study was kindly supplied by DuPont-Mitsui Fluorochemicals Co., Ltd. The PFA polymer used in this study is a random copolymer with perfluoroethylvinylether co-monomer content of 5 wt%. The PFA / organo-clay hybrids with a clay content of 5 wt%, correspondingly were coded as S1 (PFA / organo-smectite), S2 (PFA / organo-mica), and S3 (PFA / organo-mica), respectively (see table 1). These hybrids were prepared with an intensive mixer by mechanical kneading at 320 °C. In the case of melt-compounding of S3, extremely higher shear force than that of S2 case applied to the samples.

Table 1 Materials used in this study.

Samples	Component	Filler content	Comments
PFA		—	$-\text{[CF}_2\text{-CF}_2\text{]}_n\text{-[CF}_2\text{-CF(OCF}_2\text{CF}_3\text{)]}_m\text{-}$
Organo-Smectite		—	Surface treated by dimethyl dioctadecyl phosphate
Organo-Mica		—	Surface treated by dimethyl dioctadecyl phosphate
S1	PFA + organo-smectite	5 wt%	
S2	PFA + organo-mica	5 wt%	
S3	PFA + organo-mica	5 wt%	applying stronger shear force than NC2
PSN1	PFA + porous silica	3 wt%	
PSN2	PFA + porous silica	15 wt%	

PFA / porous silica hybrids were kindly supplied by Prof. K. Takeda and Dr. M. Tanahashi laboratory, Nagoya University, as comparable materials.¹³ The PFA / porous silica hybrids used in this study were abbreviated as PSN1 and PSN2 with a different filler content (see table 1).

2.2 Characterization

2.2.1. Transmission electron microscopy (TEM)

To clarify the crystallite morphology for PFA / nano-filler hybrids and the dispersed state of clay particles in the PFA matrix, we observed both the free surface (for two-step replication mode) and the cross-section (for ultramicrotome mode) of the annealed hybrid samples. In the surface replica mode, a thin cellulose acetate (CA) film wetted with small amount of methyl acetate (MA) solvent (99.5 %, Kanto-Kagaku Reagent Co. Ltd) was forced to contact with the free surface of the sample in order to produce an adequate replica. The replica was then stripped from the sample and

subjected to shadowing with Au/Pd alloy at an oblique angle of 30° in a vacuum evaporator (JEOL, JEE-400). After carbon coating and dissolving the CA film by MA, the metal-shadowed replica was transferred on TEM grids. Alternatively, thin layers of around 70 nm thick were cut from the samples at room temperature using a Reichert ultra-microtome equipped with a diamond knife. No shadowing was conducted for these microtomed samples. Both replica and microtomed samples were observed by use of a transmission electron microscope (TEM, Philips, CM-300) operated at an accelerating voltage of 200 kV.

2.2.2 Thermal analysis

The crystallization temperature (T_c) and the melting temperature (T_m) of neat PFA and the composite samples were determined using a differential scanning calorimeter (Seiko DSC-200). The instrument was calibrated with indium before the measurements. In each DSC run, a sample of about 5.00 mg was heated under a N_2 atmosphere from -10 °C up to 370°C at a heating rate of 10 °Cmin⁻¹.

2.2.3. Small-angle X-ray scattering (SAXS)

The crystalline morphology of the PFA / nano-filler hybrids was characterized with a SAXS instrument (M18XHF, MAC Science Co.) consisting of a 18 kW rotating-anode X-ray generator with a Cu target (wavelength, $\lambda = 0.154$ nm) operated at 50 kV and 300 mA. This instrument had a pyrographite monochromator, a pinhole collimation system ($\phi \sim 0.3, 0.3, 1.1$ mm), a vacuum chamber for the scattered beam path, and a two-dimensional imaging plate detector (DIP-220). The sample-to-detector distance was adjusted to 710 mm.

2.2.4. Wide-angle X-ray diffraction (WAXD)

The structural characteristics of the clay particles dispersed in the composite samples were characterized with a RAD-rA diffractometer (RIGAKU Co.). Ni-filtered $\text{CuK}\alpha$ radiation (wavelength, $\lambda = 0.154$ nm) was generated at 40 kV and 100 mA. In a $\theta - 2\theta$ mode, the samples were scanned by use of a step-scanning method with the step-width of 0.02° and 4-s intervals for the diffraction angle 2θ in the range 1.8-40°. The diffracted X-ray beam was monochromatized by a pyrographite monochromatic system and monitored by a scintillation counter.

3. RESULTS AND DISCUSSION

Figure 1 shows the TEM images of the newly prepared fluoropolymer / nano-filler composites. From the result of this observation, differences in dispersion state depended on the filler species were shown. In Figs. 1(a), 1(b), and 1(c), morphologies of PFA / organo-clay nanocomposites were presented. There were aggregated fillers of organo-modified smectite in PFA polymer matrix of composite. On the contrary, homogeneous dispersion of organo-clays were confirmed in PFA / organo-mica clay nanocomposites shown in Figs.

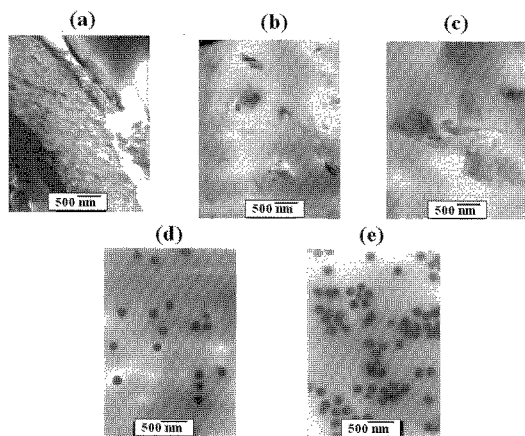


Figure 1 TEM images of fluorinated copolymer /nano-filler composites; (a) S1, (b) S2, (c) S3, (d) PSN1, and (e) PSN2.

1(b) and 1(c). Further, in Figs. 1(d) and 1(e), morphologies of PFA / porous silica nanocomposites were shown. In the comparison of these two figures, both inorganic fillers are also dispersed homogeneously in spite of differences in filler contents.

From the functional point of view in representative S2 sample, N_2 gas barrier performance (150%), shortage modulus G' (200%), and ratio of expansion (300%) are improved to the neat PFA. We supposed that these improvements of macroscopic material properties originated formation of microstructure in fluorinated nanocomposites. Therefore, fine structure estimation at nanometer and sub-nanometer size was carried out by SAXS and WAXD as follows.

Figure 2 shows the SAXS patterns and profiles of neat PFA and PFA / nano-filler composites. From the analysis of SAXS patterns, it is found that existence of long spacing values was confirmed in PFA and PFA matrix in their composites. Generally, Polytetrafluoroethylene (PTFE; $(-CF_2-CF_2)_n$) easily form rigid helices to yield extended-chain crystals.¹⁴ Consequently, there is almost no lamellar interface (crystalline/amorphous interface) in PTFE crystal. The long period values estimated by SAXS reflect existence for difference of density of between crystalline and amorphous regions. In conclusion, it finds that PFA and their composites form the lamellar crystal with folded main-chains. In Fig 2, since detective limit of this measurement is about 34 nm, values of long periods for S3, PSN1, and PSN2 samples are not correctly detected. Generally, lamellae thickness of hydrogenated crystalline polymers, such as polyethylene, polypropylene, and syndiotactic polystyrene are about 10 nm. Therefore, from the results of these SAXS measurements, fluorinated copolymers form the thicker lamellae than general hydrogenated crystalline polymers. However, crystallization degrees of PFA and their nanocomposites exhibit almost 50 % estimated by DSC measurements using ΔH value of PTFE as standard. In

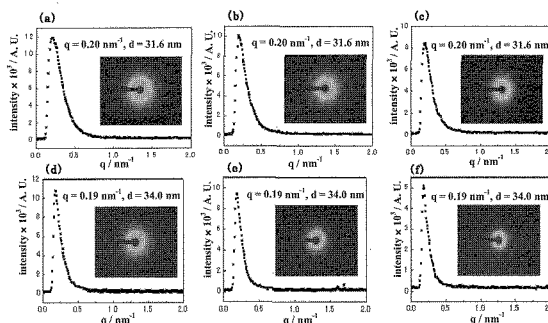


Figure 2 SAXS patterns and profiles of fluorinated copolymer /nano-filler composites; (a) neat PFA, and (b) S1, (c) S2, (d) S3, (e) PSN1, and (f) PSN2.

addition, considering only about a digit percentage of the ether comonomer component in PFA, main-chains of PFA is hard to form regular sharp folded chain and relatively small amorphous region in solid. Probably, PFA and PFA matrix in nanocomposites form switch-board type lamellae crystal with large amorphous region about 10 nm thickness.¹⁴

Figure 3 shows the WAXD profiles of neat PFA and PFA / nano-filler composites. In Fig. 3(a), the comparison between PFA / organo-smectite nanocomposites and their raw materials was shown. In the profile of composites, (001) and (002) peaks in organo-smectite which mean formation of layer structure remarkably decrease and almost disappeared. Hence, it seems that layer structure is extremely disordered in aggregates of PFA / organo-smectite nanocomposites. On the other hand, both (001) and (002) peaks are commonly confirmed in PFA / organo-mica nanocomposites, as shown in Fig. 3(b). Still now, 'intercalated structure' of polymer chains into clay galleries is common recognition of PCHs structure. Generally, this structure is confirmed by expanse of interlayer spacing of clays based on (001) peak shift of the WAXD

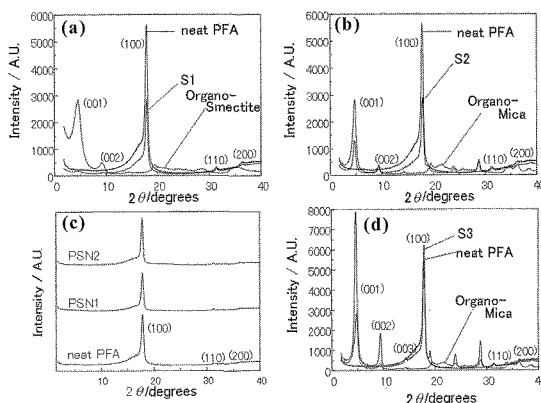


Figure 3 WAXD profiles fluorinated copolymer /nano-filler composites; (a) comparison on neat PFA, organo-smectite, and their composite, (b) comparison on neat PFA, organo-mica, and their composite, (c) comparison on neat PFA, PFA / porous silica (3 wt%), and PFA / porous silica (15 wt%) hybrids, (d) comparison on neat PFA, organo-mica, and their composite applied by strong shear force.

profiles. In this case, fluorinated polymer chain can not intercalate clay galleries because of no shift of (001) peaks. The immiscibility between fluorinated and hydrogenated compounds is well-known. It is guess that there is poor affinity between fluorinated polymer chain and surface treated alkyl chain in clay surface.

The intensities of (100) reflection peaks came from of quasi-hexagonal PFA matrix are obviously decreased in both organo-smectite (Fig. 3(a)) and organo-mica (Fig. 3(b)) nanocomposites. This experimental fact means that crystallinity of both hybrids is relative lower than neat PFA itself. In the point of view on crystallinity of PFA matrix, PFA / porous silica hybrids indicate extremely interesting property. Independently on the filler contents, the (100) peak intensity of PFA exhibited almost unchanging between neat PFA and their silica composites. In addition, matrix crystallinity of PFA / organo-mica nanocomposites applied the strong shear force on the formation process is rather higher than neat PFA (Fig. 3(d)). From higher intensity of (001) peak in WAXD profile of S3, regularity of layer structure of organo-clay in this composite is also improved. In the control of structure from the nanometer level, an application of shear force on formation process of composites is important things related to control of crystallinity for materials. Further, melting peaks of PFA / porous silica nanocomposites in DSC thermograms were obviously shifted to higher temperature side than that of neat PFA. The origin of this thermal behavior corresponds to the occurrence for nucleator effect of silica to the matrix PFA.

Figure 4 shows the schematic illustrations of structure of S2 type for PFA / organo-mica nanocomposite, and nucleation process of PFA matrix in PFA/porous silica nanocomposites. In the PFA/clay nanocomposites, PFA matrix formed lamellar structure with folded chain and fluorinated polymer chain can not intercalate in to clay galleries (Fig. 4 (a)). The part of chain-holding always contains the ether side-chain units, and long period value between lamellar gravity is about 32 nm thickness. These microstructure formations of PFA nanocomposites contribute the improvements for material properties. Further, in the case of PFA / silica composites, the values of fusion enthalpy ΔH_f are increased by the twice value to the neat PFA, and reached to 32 mJ/mg. The shape of melting peak in thermograms extremely became sharp. This characteristic thermal behavior is based on the adsorption of the polymer chain to the porous silica surface. That is to say, silica plays a role as nucleation agent to the fluoropolymers in these nanocomposites. These models of microstructure are supported by both WAXD and DSC data.

As mentioned previously, PFA / nano-filler composites reported in this paper formed characteristic microstructure from the nanometer

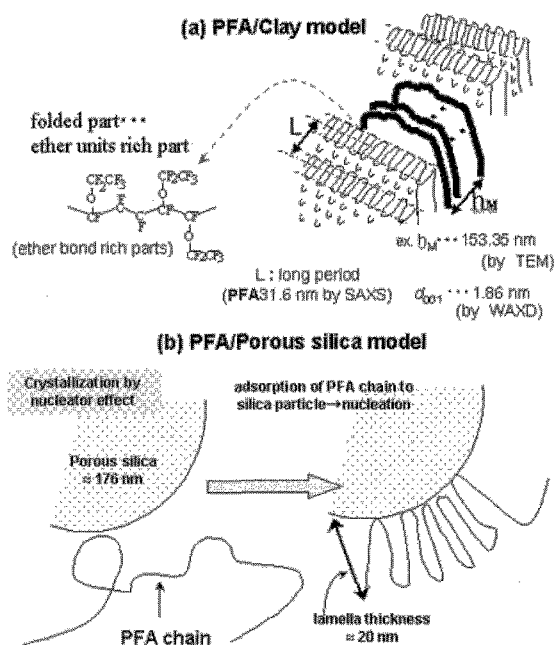


Figure 4 Schematic models of fluorinated copolymer /nano-filler composites; (a) S2 and (b) PSN samples.

or sub-nanometer sizes to the bulk levels. The formation of these 'hierarchical structures' may bring an excellent physical property and interesting thermal behavior.

REFERENCES

- [1] P. C. LeBaron, Z. Wang, T. PinrLavaia, *J. Appl. Clay Sci.* **15**, 11, (1999).
- [2] M. Alexandre, P. Dubois, *Mater. Sci. Eng.*, **28**, 1, (2000).
- [3] P. Messersmith, E. P. Giannelis, *J. Polym. Sci., Polym. Phys.* **33**, 1047, (1995).
- [4] A. Usuki, Y. Kojima, A. Okada, Y. Fukushima, T. Kurauchi, O. Kamigaito, *J. Mater. Res.*, **8**, 1179, (1993).
- [5] N. Ogata G. Jimenez H. Kawai, T. Ogihara, *J. Polym. Sci., Polym. Phys.* **35**, 389, (1997)
- [6] R. Vaia. H. Ishii, E. P. Giannelis, *Chem. Mater.*, **5**, 1694, (1993).
- [7] R. Vaia, K. D. Jandt, E. J. Kramer, E. P. Giannelis, *Macromolecules*, **28**, 8080, (1995).
- [8] H. R. Dennis, D. L. Hunter, D. Chang, S. Kim, J. White, J. W. Cho, D. R. Paul, *Polymer*, **42**, 9513, (2001).
- [9] J. C. Lee, S. Namura, S. Kondo, A. Abe, *Polymer*, **42**, 8631, (2001).
- [10] R. M. Overney, E. Meyer, J. Frommer, H. J. Güntherodt, *Langmuir*, **10**, 1281, (1994).
- [11] C. W. Burn, E. R. Howells, *Nature*, **18**, 549, (1954).
- [12] J. Burdon, J. C. Tatlow, "Advances in Fluorine Chemistry," Vol. 1 (eds. M. Stacey, J. C. Tatlow, A. G. Sharp, Academic Press, New York, 1960), pp.129-165.
- [13] M. Tanahashi, M. Hirose, J. C. Lee, K. Takeda, *Polym. Adv. Technol.*, **17**, 981, (2006).
- [14] A. Fujimori, M. Hasegawa, T. Masuko, *Polym. Int.*, **56**, 1281, (2007).